Expanded Flight & Ground Testing Data Set for an Unmanned Aircraft: Great Planes Avistar Elite

3 authors, including:

Or Dantsker
University of Illinois, Urbana-Champaign

48 PUBLICATIONS   **437** CITATIONS

Renato Mancuso
Boston University

80 PUBLICATIONS   **1,428** CITATIONS

Some of the authors of this publication are also working on these related projects:

Software-Shaped Platforms View project

General Aviation Upset and Stall Aircraft Recovery View project

Expanded Flight & Ground Testing Data Set for an Unmanned Aircraft: Great Planes Avistar Elite

Or D. Dantsker* and Marco Caccamo †

Technical University of Munich, Garching, Germany

Renato Mancuso‡

Boston University, Boston, MA 02215

This paper presents the recently expanded flight and ground testing data set for a trainer-type unmanned aircraft, the Great Planes Avistar Elite. This is in the series of aircraft data sets that are being published online and freely available as part of the Unmanned Aerial Vehicle Database (UAVDB). The database is being continually expanded including aircraft and their components (e.g. propellers) as they are tested. This paper includes ground measurement, aircraft modeling, and flight testing results. Specifically, ground testing includes 3D scanning of geometry, moment of inertia testing, and propeller performance testing. Aircraft modeling includes a Solidworks CAD model, computational aerodynamics tool models in AVL, XFLR5, and Fluent, a propulsion system power model, and a flight simulation model in the X-Plane flight simulator. Flight testing results as well as testing and setup techniques are presented. Additionally, details regarding aircraft construction and instrumentation are provided.

Nomenclature

CAD	=	computer aided design	n	=	propeller and motor rotation rate
CFD	=	computational fluid dynamics	p, q, r	=	roll, pitch and yaw rotation rates
$COTS$	=	commercial-off-the-shelf	R_m	=	internal motor resistance
DOF	=	degree of freedom	S	=	wing area
ESC	=	electronic speed controller	u, v, w	=	body-fixed true velocity
GPS	=	global positioning system	U_m	=	motor terminal voltage
IMU	=	inertial measurement unit	V	=	total speed
PWM	=	pulse width modulation	x, y, z	=	position in ENU coordinate system
UAV	=	unmanned aerial vehicle			
			α	=	angle-of-attack
a_x, a_y, a_z	=	body-axis translational acceleration	β	=	sideslip angle
c	=	wing mean chord	γ	=	climb angle
C_{D_o}	=	parasitic drag coefficient	η_{ESC}	=	ESC efficiency
g	=	gravitational acceleration	η_{motor}	=	motor efficiency
i_0	=	zero load motor current	$\eta_{propeller}$	=	propeller efficiency
K_i, K_p	=	propulsion model constants	ϕ, θ, ψ	=	roll, pitch and heading angles
K_v	=	motor speed constant	ρ	=	density of air
m	=	aircraft mass			

I. Introduction

In recent years, we have seen an uptrend in the popularity of unmanned aerial vehicles (UAVs) driven by the desire to apply these aircraft to a variety of civilian, commercial, education, and government applications. Part of this uptrend in UAV use includes increase in the research related to them. There have been UAVs used to study

---

*Researcher, TUM School of Engineering and Design, or.dantsker@tum.de

†Professor, TUM School of Engineering and Design, mcaccamo@tum.de

‡Assistant Professor, Department of Computer Science. rmancuso@bu.edu

American Institute of Aeronautics and Astronautics

aerodynamic qualities,[1,2] especially in high angle-of-attack conditions.[3–5] Others have been used as testbeds to develop new control algorithms.[6–9] Additionally, some unmanned aircraft are used as low-cost stand-ins for experiments that are too risky or costly to perform on their full scale counterparts, i.e. stall or upset maneuvers.[10–14] In addition, new aircraft configurations[15–18] and flight control hardware and software[19–23] have been tested. Research evaluating aircraft power consumption reduction through steady and dynamic soaring has also become the subject of significant attention recently.[24–28]

Broadly, development of a UAV platform takes several stages.[29–32] First the airframe must be developed, which may involve design creation and construction, in the case with a custom design, or just construction, in the case of an already designed and pre-constructed commercial-off-the-shelf airframe (often a model aircraft kit). Next, instrumentation will follow a similar development route, depending on whether it is custom or commercial-off-the-shelf. Then comes ground testing, which may involve loads testing, moment of inertia measurement, and pre-flight combined systems testing. In summation, these stages become extremely costly in terms of resources as well as time. A research group may spend many months or possibly years to develop an aircraft, which may only be flight tested for a limited time.

This paper presents a flight and ground testing data set for a trainer-type unmanned aircraft, a Great Planes Avistar Elite,[33] which can be seen in Figure 1. This is the second of a series of aircraft that are being published online and freely available as part of the Unmanned Aerial Vehicle Database[34] (UAVDB)[a].This paper includes ground measurement, aircraft modeling, and flight testing results. First, details regarding aircraft construction and instrumentation are provided. Then, ground testing including 3D scanning of geometry, moment of inertia testing, and propeller performance testing are presented. After that, aircraft modeling including a Solidworks CAD model, computational aerodynamics tool models in AVL, XFLR5, and Fluent, a propulsion system power model, and a flight simulation model in the X-Plane flight simulator are shown. Finally, an overview of flight testing results as well as testing and setup techniques using a flight testing automation tool[35] is given.

Figure 1: The flight-ready instrumented Great Planes Avistar Elite.

II.   Aircraft Description

The Great Planes Avistar Elite is a commercial-off-the-shelf (COTS) model aircraft designed for radio control flight training.[33] Specifically, the aircraft has a fixed high-wing configuration and is primarily constructed from wood and plastic film covering. Top, bottom, left, and right views are shown in Fig. 2. Given the aircraft's ease of construction and operation, robustness, and re-configurablity, it has made an excellent UAV research testbed.[36–42]

---

[a]UAVDB is published online at www.uavdb.org and includes other aircraft such as a 26%-scale Cub Crafters CC11-100 Sport Cub S2.[?,34]

American Institute of Aeronautics and Astronautics

Figure 2: Top, bottom, left, and right views of the Great Planes Avistar Elite with an the internal combustion engine [image taken from Great Planes[33]].

A.   Aircraft Construction

The major airframe components of the Great Planes Avistar Elite are shown in Fig. 3. The aircraft was designed to be propelled with either a nitro internal combustion engine or an electric motor; the latter was chosen for this work as it provides near constant performance, increased reliability, and low vibrations. The aircraft was constructed mainly following manufacturer recommendation with the exception some small improvements to the control surface actuator linkages and propulsion system. Detailed photos of the aircraft in the as-built configuration are shown in Fig. 4.Airframe specifications are provided in Tables 1 and 2.
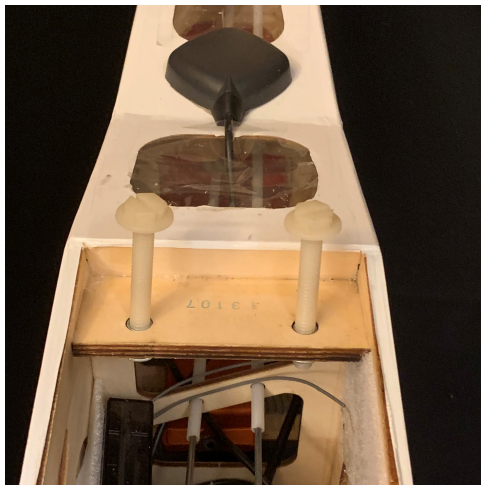

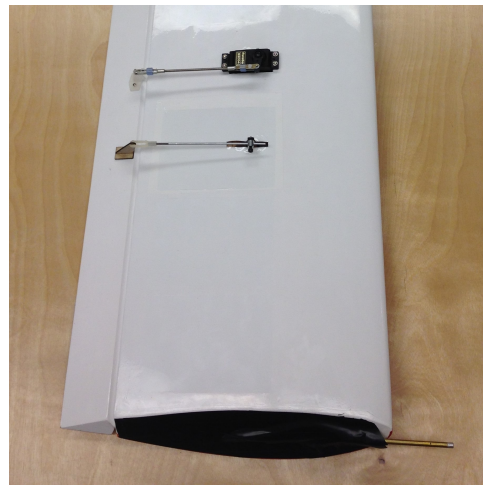Figure 3: The major airframe components of the un-built Great Planes Avistar Elite [image taken from Great Planes[33]].

American Institute of Aeronautics and Astronautics
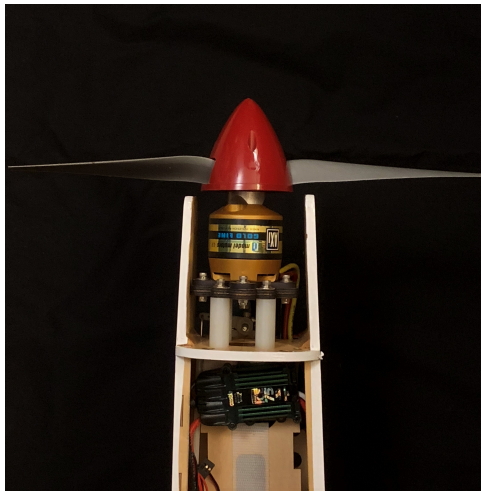
Figure 4: Key aircraft details of the as-built instrumented Great Planes Avistar Elite: (a) nose of aircraft with brushless motor, propeller, and ESC, (b) integrated Hall-effect current sensor next to the ESC, (c) rear of fuselage behind wing mounting location containing the inertial measurement unit (IMU) mounted inside and the GPS antenna ontop, and (d) outer wing with aileron servo and pitot probe.

B. Instrumentation

The Great Planes Avistar Elite aircraft was instrumented with an Al Volo FC+DAQ[43] data acquisition system. The system operates at 400 Hz and integrates with a 9 degree-of-freedom (9-DOF) XSens MTi-G-710[44] IMU with a GPS receiver. The pilot commands are also recorded by measuring the pulse width modulation (PWM) signals generated by receiver. The propulsion system information is logged by FDAQ through an interfaces with the Castle Creations Edge 75A ESC; recently, an integrated Hall-effect current sensor was added between the ESC and the battery to monitor current input. Using the sensors, the system is able to log and transmit: 3D linear and angular accelerations, velocities, and position along with GPS location; pitot-static probe airspeed; 3D magnetic field strength and heading; control surface deflections; and propulsion system voltage, motor and ESC current, RPM, and power. Specifications for the instrumentation can be found in Table 3.

Table 1: Airframe physical specifications.

Geometric Properties	
Overall Length	55.0 in (1395 mm)
Wing Span	62.5 in (1590 mm)
Wing Area	672 in^2 (43.3 dm^2)
Aspect Ratio	6.62
Inertial Properties	
Weight	
Empty (w/o Batteries)	6.77 lb (3.07 kg)
Batteries	1.39 lb (0.63 kg)
Gross Weight	8.16 lb (3.70 kg)
Wing Loading	28.0 oz/ft^2 (85.5 gr/dm^2)

Table 2: Airframe component specifications.

Construction	Built-up balsa and plywood structure, aluminum wing tube, aluminum landing gear, abs canopy, and plastic film sheeted.
Flight Controls	
Controls	Aileron (2), elevator, rudder, throttle, and flaps (2)
Transmitter	Futaba T14MZ
Receiver	Futaba R6014HS
Servos	(6) Futaba S3004
Regulator Distribution	Castle Creations CC BEC
Receiver Battery	Thunder ProLiteX 25c 2S 7.4V 450 mAh
Propulsion	
Motor	Model Motors AXI 4120/14 Outrunner
ESC	Castle Creation Phoenix Edge 75 Amp Brushless Speed Controller
Propeller	Landing Products APC 13x8E
Motor Flight Pack	Thunder Power ProLiteX 25c 4S 14.8 V 6 Ah lithium polymer battery

Table 3: Instrumentation specifications.

Data acquisition system	Al Volo FC+DAQ 400 Hz system
Sensors	
Inertial measurement unit	XSens MTi-G-710 AHRS with GPS
Airspeed sensor	Al Volo Pitot Static Airspeed Sensor
Motor sensor	Al Volo Castle ESC Interface
Current sensor	Allegro Hall-Effect Current Sensor
Power	
Regulator	Built into FC+DAQ
Battery	Thunder Power ProLiteX 25c 3S 11.1 V 1350 mAh lithium polymer battery

American Institute of Aeronautics and Astronautics

III. Ground Measurement and Testing

To date, the Great Planes Avistar Elite aircraft and its components have been extensively measured and ground tested. This includes 3D scanning of the entire aircraft,[45] moment of inertia testing,[39] and propeller performance testing.[46]

A. 3D Scanning

The 3D scanning was performed using a ZCorporation ZScanner 800 self-positioning handheld 3D scanner. The 3D point cloud output from the scanner was processed using a previously written MATLAB script called AirplaneScan. The points on the right half of the airplane were discarded, and then the points on the left half were mirrored to the right with the exception of the nose gear, which was not mirrored.The resulting processed 3D point cloud can be seen in a 3-view and an isometric view in Fig. 7. The processed point cloud was then sliced multiple times to yield the cross sections of the fuselage, wings, and tail sections, which can be found in related work.[45]

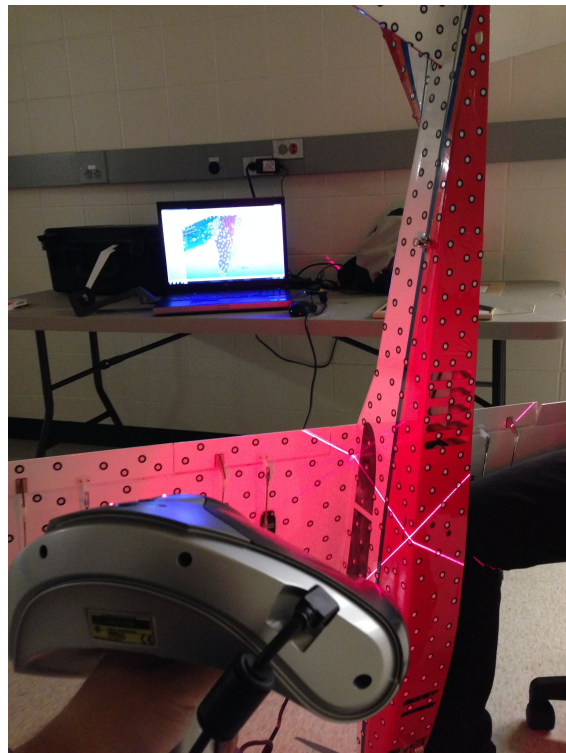Figure 5: The Great Planes Avistar Elite being 3D scanned from above.

Figure 6: The Great Planes Avistar Elite being 3D scanned from below.

The pointcloud slices generated by the AirplaneScan MATLAB script provided dimensions and coordinates for all of the flight surfaces. It is important to note that the wing has the same airfoil along the wingspan and the empennage surfaces each have continuously varying airfoils from root to tip. The coordinates of each airfoil produced are plotted in Fig. 8. The wing airfoil coordinates were verified[45] with coordinates for the AVISTAR airfoil found on the UIUC Airfoil Database,[47] as can be seen in Fig. 9, and the stabilizer airfoils were verified with manual measurements. The dimensions of each flight surface and the airfoil locations are given in Table 4; the coordinate system used has the x-axis towards the tail, the y-axis towards the right wing, and the z-axis up.

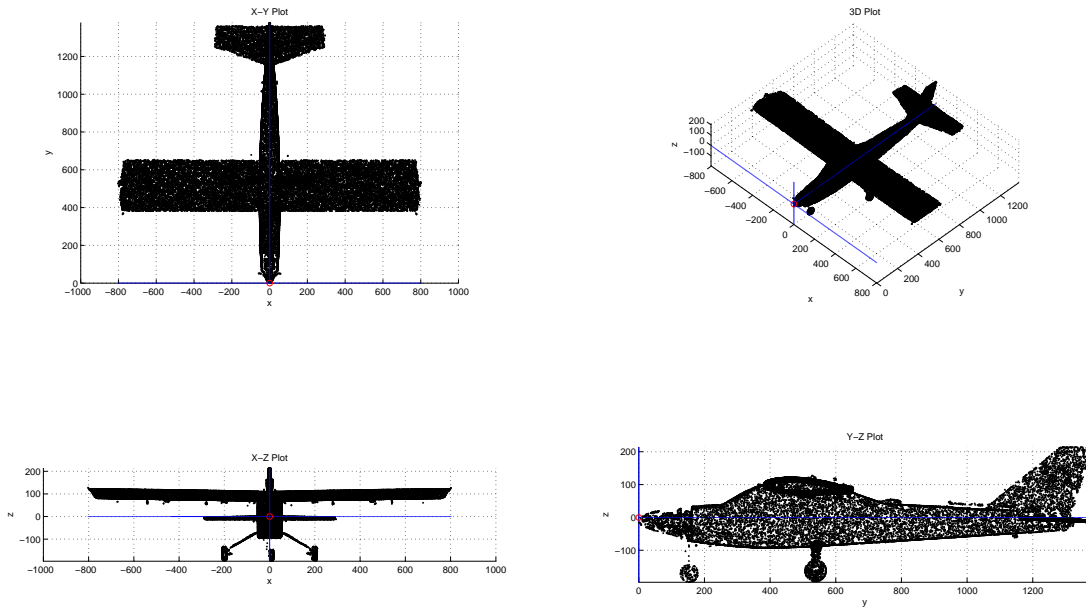American Institute of Aeronautics and Astronautics

Figure 7: 3-view and isometric plots of the Great Planes Avistar Elite scan 3D point cloud after processing.
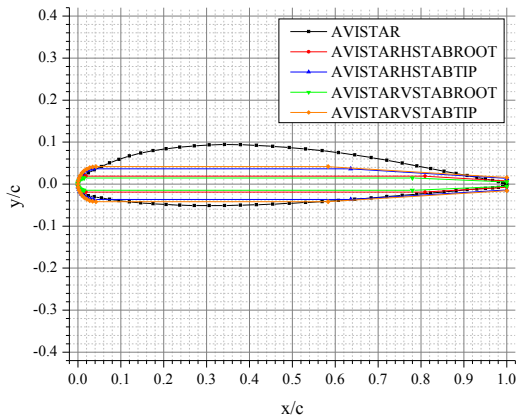

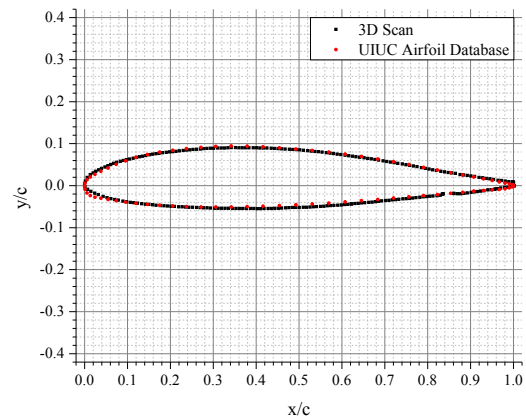Figure 8: The airfoils used on the Great Planes Avistar Elite.

Figure 9: Comparison of AVISTAR airfoil coordinates between the 3D scan and UIUC Airfoil Database.

Table 4: Avistar UAV flight surface specifications.

Wing							
LE x pos	LE z pos	Incidence	y span pos	Chord	Offset	Dihedral	Airfoil
380.4 mm	95.5 mm	3.58 deg	0 mm	237.10 mm	0 mm	0.9 deg	AVISTAR
-	-	-	793.75 mm	237.10 mm	0 mm	-	AVISTAR
Horizontal Stabilizer							
LE x pos	LE z pos	Incidence	y span pos	Chord	Offset	Dihedral	Airfoil
1160 mm	-2.04 mm	2.36 deg	0 mm	210 mm	0 mm	0 deg	AVISTARHSTABROOT
-	-	-	291 mm	110 mm	100 mm	-	AVISTARHSTABTIP
Vertical Stabilizer							
LE x pos	LE z pos	Incidence	y span pos	Chord	Offset	Dihedral	Airfoil
1160 mm	17.96 mm	2.36 deg	0 mm	273 mm	-95 mm	0 deg	AVISTARVSTABROOT
-	-	-	200 mm	96 mm	133 mm	-	AVISTARVSTABTIP

American Institute of Aeronautics and Astronautics

B. Moment of Inertia Testing

Moment of inertia measurement of the flight-ready, instrumented Great Planes Avistar Elite aircraft was performed using a moment of inertia testing rig developed in previous work. A new mounting system was developed that hard mounts the aircraft to accurately measure values for all there axes. Note that due to the mounts, certain components, e.g. main landing gear, were tested separately, and that calibration of the mounts on their own is used to remove their inertia from the results. Photos of the testing are shown below in Fig. 10. Testing results, as well as raw data, can be found online on UAVDB. A thorough explanation of the process can be found in the previous literature.[39]

(a)

(b)

(c)

(d)

Figure 10: Moment of inertia testing of the flight-ready, instrumented Great Planes Avistar Elite about the (a) roll axis, (b) yaw axis, and (c-d) pitch axis.

American Institute of Aeronautics and Astronautics

C.   Propeller Performance Testing

As presented in Table 2, the propulsion system on the Great Planes Avistar Elite consists of an Landing Products APC 13x8E propeller,[48] Model Motors AXI 4120/14 brushless outrunner motor, Castle Creations Phoenix Edge 75 electronic speed controller, and a Thunder Power ProLiteX 25c 4-cell, 14.8 V 6 Ah lithium polymer battery. Propeller performance testing of the APC 13x8E propeller was conducted in the UIUC low-turbulence subsonic wind tunnel[46] using the equipment and procedures outlined in the literature.[49] Results are shown in Fig. 11 and 12 under freestream conditions at rotation rates between 3,000 and 7,000 RPM and static at rotation rates between 1,000 and 7,500 RPM, respectively. Testing results for the APC 13x8E propeller, as well as of several other propellers that could be used on the Great Planes Avistar Elite, are available on UAVDB and the UIUC Propeller Database[50]
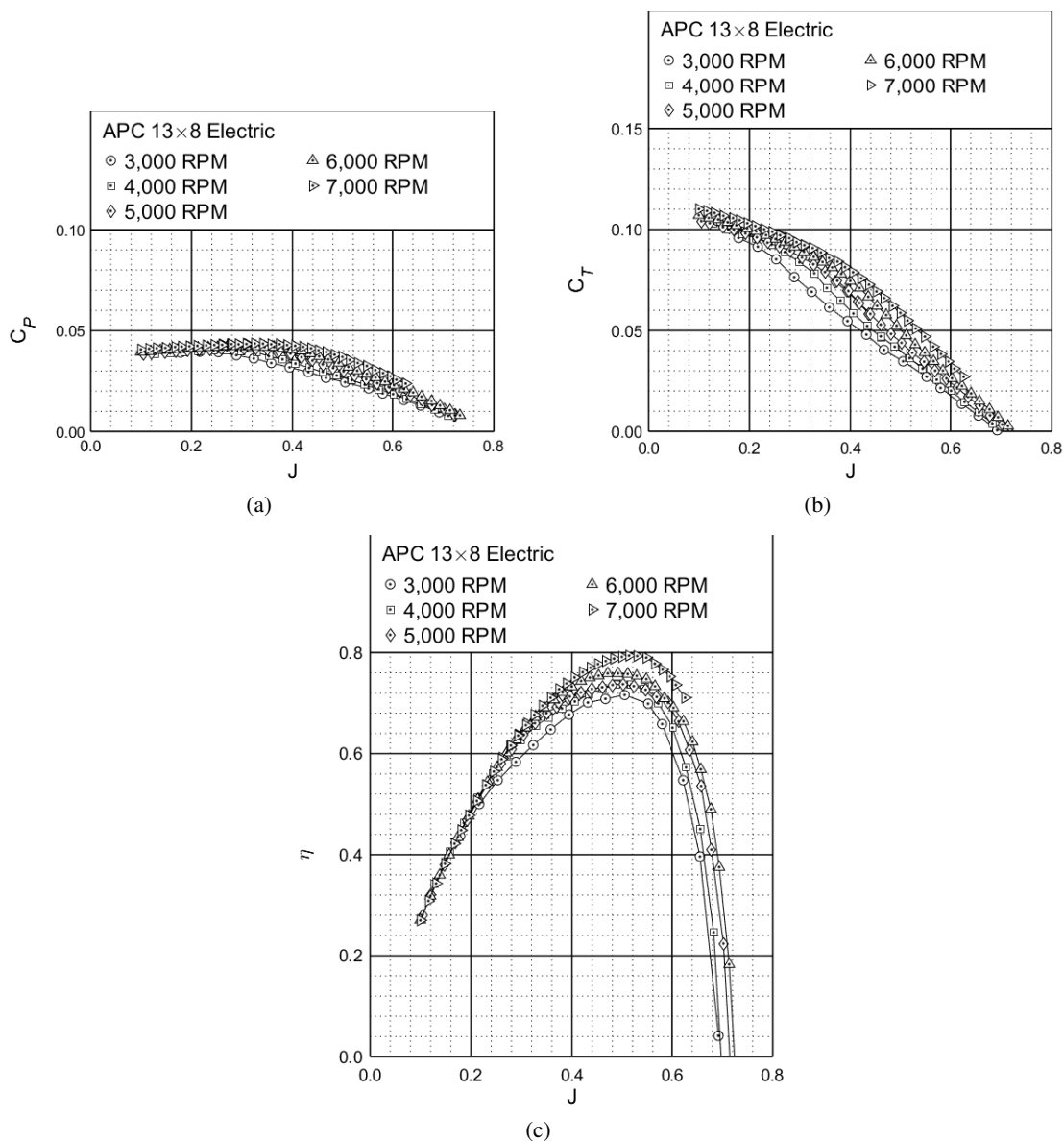

(a)

(b)

(c)

Figure 11: Performance of the APC 13×8 Thin Electric propeller: (a) thrust coefficient, (b) power coefficient, (c) efficiency.

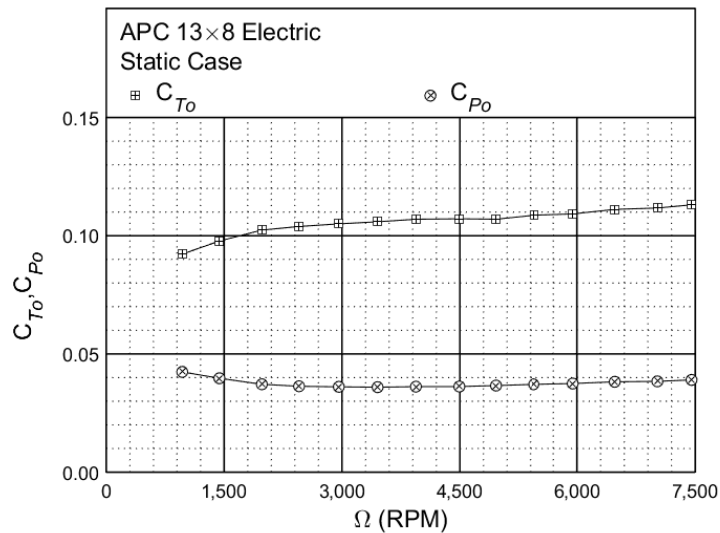American Institute of Aeronautics and Astronautics

Figure 12: Static performance of the APC 13×8 Thin Electric propeller: thrust and power coefficient.

IV. Aircraft Modeling

A slew of digital models have been created for the Great Planes Avistar Elite aircraft based on ground and flight test measurements. These include a CAD model in Solidworks, several computational aerodynamic tool models,[51] a propulsion system power model,[40] and a flight simulation model[32] in X-Plane.

A. CAD Model

A Solidworks CAD model was developed for the Great Planes Avistar Elite using 3D geometry data collected from the aforementioned 3D scan. Specifically, the fuselage shape was directly created from the 3D scan by vertically and horizontally slicing the 3D point cloud. Meanwhile, the flight and control surfaces were created from the analyzed surface parameters presented in Table 4 and airfoil geometry presented in Fig. 8 and. The final CAD model is presented in Fig. 13.
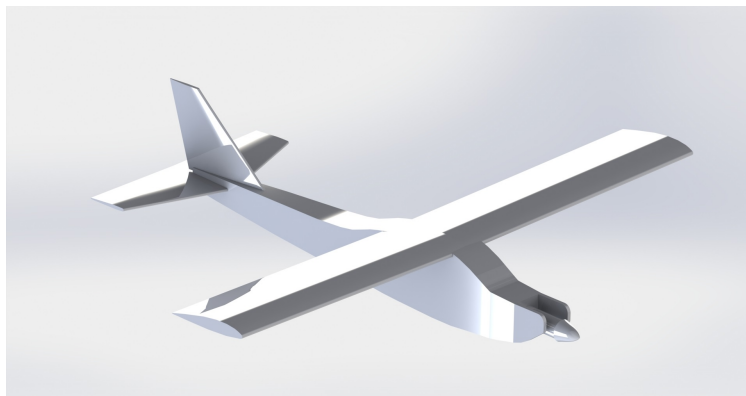

Figure 13: The SolidWorks CAD model of the Great Planes Avistar Elite.

American Institute of Aeronautics and Astronautics

B. Computational Tool Models

The 3D model of the Great Planes Avistar Elite generated using the point cloud was input into 3 types of computational tools. Two low-order computational tools based on lifting-line theory, XFLR5[52] and Athena Vortex Lattice (AVL),[53] as well as one high-order method computational fluid dynamics (CFD) tool Ansys Fluent. Photos of the 3 models are shown below in Figs. 14-16. These methods were used and compared to previous flight test campaigns with the Avistar Elite.[51] These models are publicly available for additional analysis.
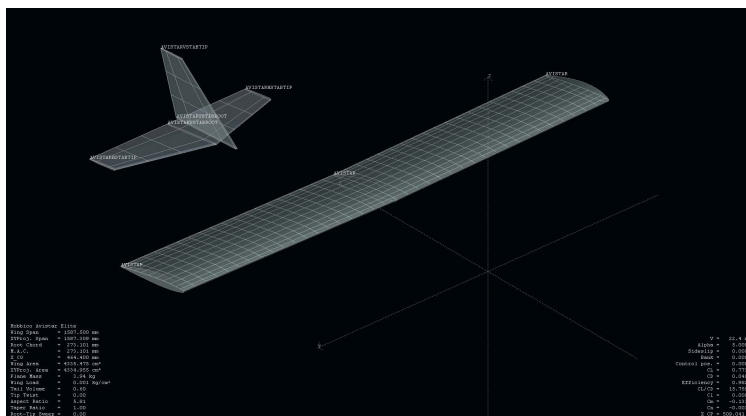

Figure 14: The XFLR5 aerodynamics model for the Great Planes Avistar Elite.
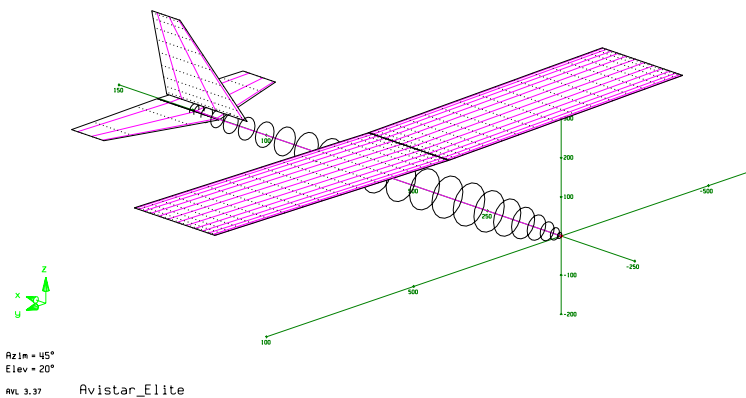

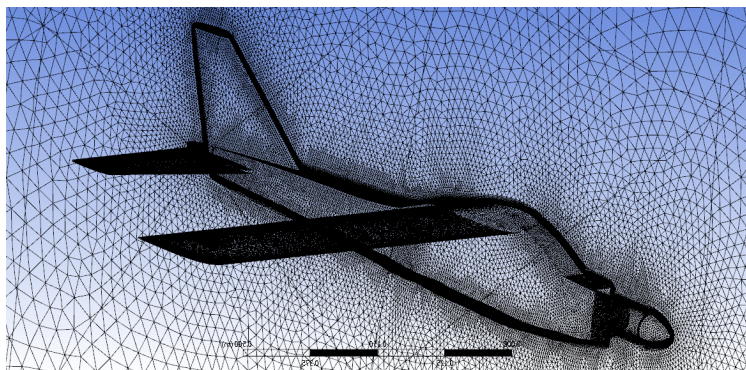Figure 15: The AVL aerodynamics model for the Great Planes Avistar Elite.

Figure 16: The Great Planes Avistar Elite CAD model meshed in Ansys Fluent with 4 million cells.

American Institute of Aeronautics and Astronautics

C. Propulsion System Power Model

A high-fidelity, low-order power consumption model for electric, fixed-wing UAVs was developed with and validated using the Great Planes Avistar Elite in related work.[40] In order to make the model as versatile as possible, state variable inputs are restricted to easily measurable values. Specifically, the variable inputs are properties of the aircraft maneuver, including velocity, acceleration, roll (bank) angle, and climb angle. Doing so requires certain assumptions[b], which work well for the overwhelming majority of UAV flight. Therefore, the power model provides an estimation based on the motion of the aircraft, i.e. flight path, with minimal knowledge of the aircraft flight mechanics attributes. Figure 17 shows how the model is cascaded from the input variables, through a flight mechanics model, a propeller model, a motor model, and an ESC model.
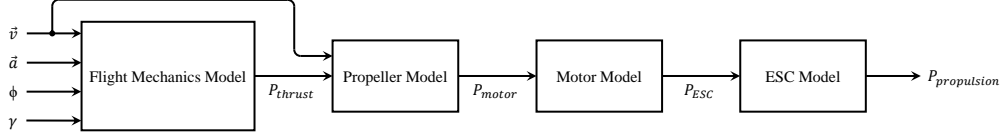

Figure 17: Aircraft propulsion power modeling based on aircraft state.

The final expression of the power model is:

$$P_{propulsion} = \frac{K_p v^3 + K_i \frac{\cos^2 \gamma}{v \cos^2 \phi} + mgv \sin \gamma + m\vec{a} \cdot \vec{v}}{\eta_{propeller} \cdot \eta_{motor} \cdot \eta_{ESC}} \tag{1}$$

where

$$K_p = \frac{1}{2} \rho S C_{D_o} \tag{2}$$

$$K_i = \frac{2K m^2 g^2}{\rho S} \tag{3}$$

Motor efficiency, η_{motor}, is found using a first order approximation by Drela,[54] propulsion system voltage, and motor parameters

$$\eta_{motor}(n, U_m) = \left(1 - \frac{i_0 R_m}{U_m - 60n/K_v}\right) \frac{60n}{U_m K_v} \tag{4}$$

Propeller efficiency, $\eta_{propeller}$, is interpolated from propeller performance data presented in Section III.C. And ESC efficiency, η_{ESC}, is found using models in literature.[55–57]

The propulsion power model was evaluated by means of flight testing using the instrumented Great Planes Avistar Elite. The aircraft was autonomously flown through a reference flight path, which contained turns, climbs, descents, and straight line segments. The flight testing showed very close agreement between the power and energy estimates determined using the power model from aircraft state data and actual experimental power and energy measurements, within less than 5%.

---

[b]It is assumed that the angle-of-attack remains relatively constant, the incidence angle is approximately zero, and thus the flight path climb angle is approximated as the measurable pitch angle. Additionally, it is assumed that there is minimal side-slip allowing for the turn radius to be calculated directly from the roll angle.

D.   Flight Simulation Model

A flight simulation model of the Great Planes Avistar Elite was developed into the X-Plane flight simulator[58] as part of the uavEE emulation environment effort.[59] The flight simulation model, which is shown in Fig. 18, was developed using the aforementioned 3D scan geometry data and CAD model. There is an ongoing effort to compare the flight behavior of the simulation model to the real-life aircraft, including assessment of stability and control derivatives; the ultimate goal of this effort is to enhance the fidelity of the simulation model in the linear regime for use in a multi-domain digital-twin environment.

Figure 18: The X-Plane flight model of the Avistar UAV.

V.   Flight Testing

Flight testing of the Great Planes Avistar Elite aircraft was conducted performing a range of maneuvers to enable characterization of aircraft aerodynamics, longitudinal and lateral stability, and control effectiveness. Specifically, flight testing was performed using a flight testing automation tool[35] to repeatedly perform these parameterizable flight testing maneuvers with minimal human error. Specifically, the maneuvers conducted include trimmed flight, stalls, singlets, and doublets and are further detailed in Table 5. This flight testing automation tool is integrated into the uavAP autopilot software[23] running on the aircraft and into the uavEE ground station software.[59]

Characterization of the aircraft using the flight testing automation tool is conducted with a pilot and an operator. The pilot manually takesoff and lands the aircraft, as well as initially sets up the aircraft for automated flight. Meanwhile, the operator monitors and commands the aircraft into preparatory holding patterns and the automated maneuvers using a ground station running uavEE.[59] In this setup, the pilot can override the autopilot at any time using the radio transmitter, in case of emergencies and for takeoff and landing. A screenshot of the ground station interface is shown in Fig. 19.

In order to conduct automated flight testing, an initial trim maneuver needs to be first performed. In this maneuver, the aircraft attempts to fly straight and level at a constant velocity within predefined steady-state noise bounds for a predefined amount of time; the control output values are averaged and the saved as trim, and used as the baseline for all maneuvers performed by the automator. For example, after an excitation (singlet or doublet), it is desired that the control surfaces be returned to level flight trim such that the un-actuated response can be recorded. It should be noted that measuring trim requires low environmental disturbances (e.g. wind, thermals, etc).

Fig. 19 shows a screenshot of the uavEE ground station interface with the aircraft performing an up-down 1000 ms, 50% elevator deflection doublet maneuver. As shown in the figure, the aircraft is setup in a holding pattern the provides

American Institute of Aeronautics and Astronautics

a consistent initial state before each maneuver. The aircraft is thus set up at the same speed and in approximately the same direction to ensure consistency. The direction of the pattern can be adjusted to accommodate for wind direction as to reduce cross wind effects, thus minimizing external β. As shown in Fig. 19, there is some crosswind present which causes each of the maneuvers paths to slightly deviate from the straight path it is set up on. Additionally, it should be noted that the placement of the setup maneuver was also positioned to maintain line of sight throughout the experiments.

51 parameterizable flight testing maneuvers were performed using the automation tool. These include trimmed level and gliding flight, stalls with varied aircraft weight, singlets for ailerons and elevator, and doublets for aileron, elevator, and rudder. Flight test data, state data time histories, and trajectory plots for each of the aforementioned maneuvers are available for download from the UAVDB website. An example aircraft state data time history and trajectory plot are shown in Fig. 20 and 21, respectively, for an aileron doublet performed by the Great Planes Avistar Elite.

Table 5: Flight Test Maneuvers Planned

| Maneuver	Variations	Description
Trimmed Flight	-	Straight and level flight at 20 m/s.
Idle Descent	-	Descent using idle power with trim for 20 m/s.
Stall	Vary aircraft weight	Starting with powered level flight at 20 m/s, the propulsion system is turned off, constant altitude is maintained until stall occurs, then centering of controls.
Aileron Singlet	Right or left, vary periods and amplitudes	Level flight followed by momentary aileron deflection and then centering of controls.
Aileron Doublet	Right-left or left-right, vary periods and amplitudes	Level flight followed by momentary aileron deflection in direction, then the other, and then centering of controls.
Elevator Singlet	Up or down, vary periods and amplitudes	Level flight followed by momentary aileron deflection and then centering of controls.
Elevator Doublet	Up-down or down-up, vary periods and amplitudes	Level flight followed by momentary aileron deflection in direction, then the other, and then centering of controls.
Rudder Doublet	Left-right or right-left, vary periods	Level flight followed by momentary aileron deflection in direction, then the other, and then centering of controls.
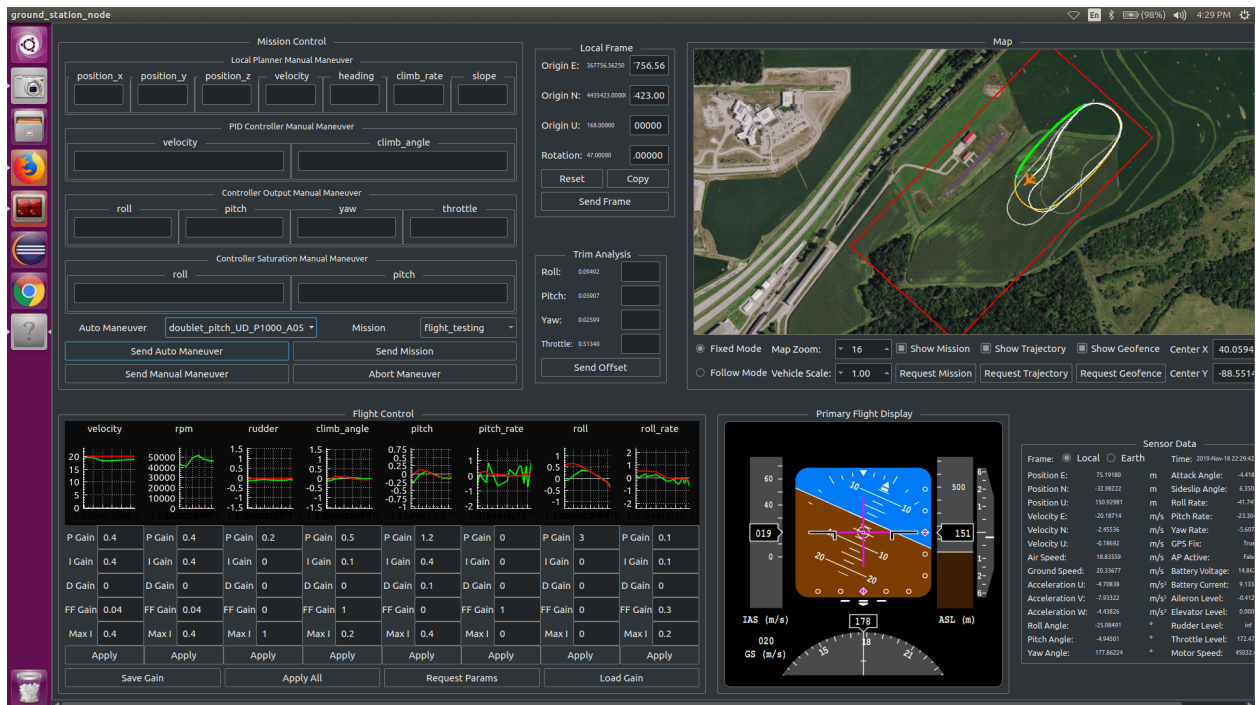
Figure 19: A screenshot of the *uavGS* interface showing a doublet performed using the flight testing automation tool.
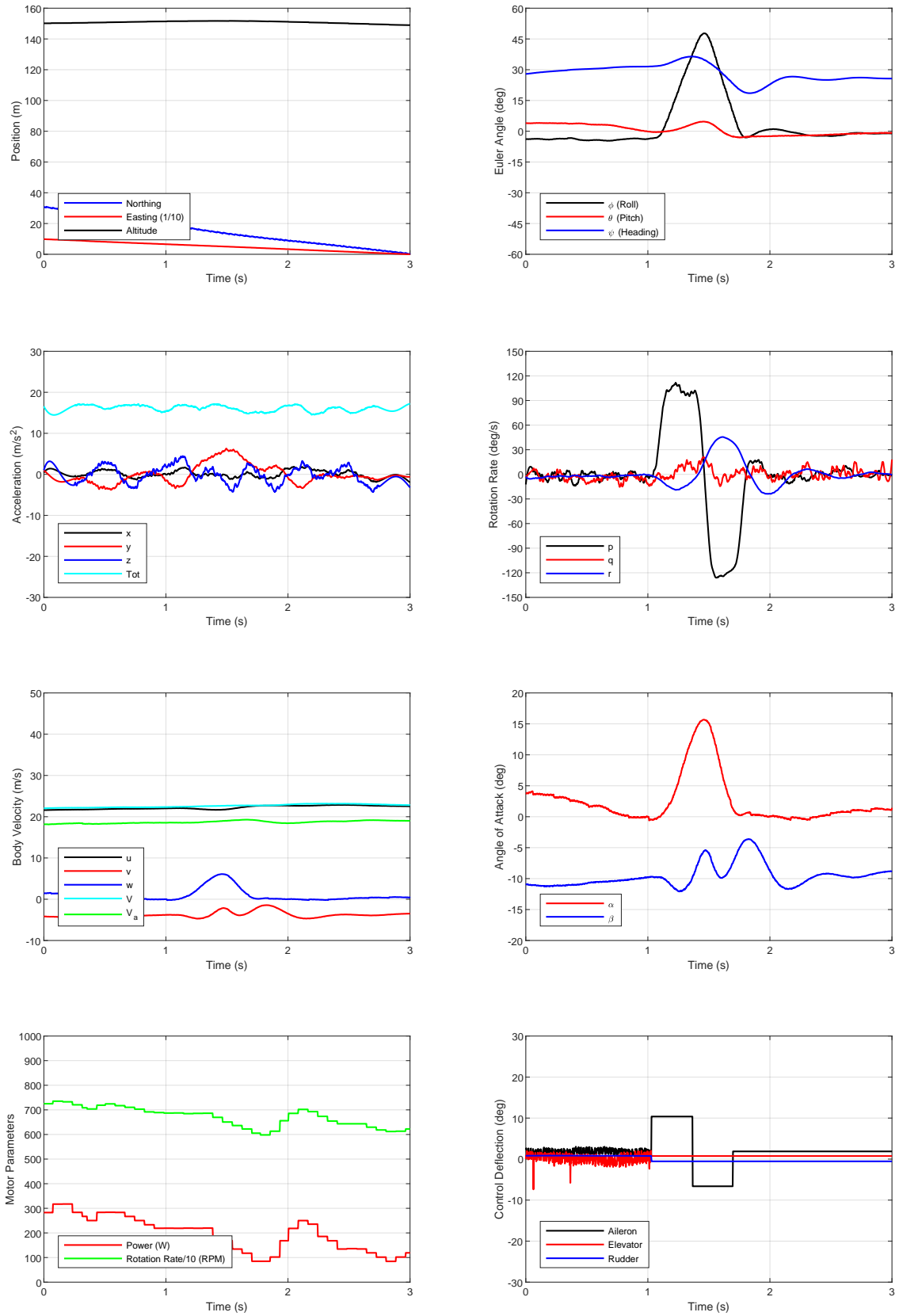
American Institute of Aeronautics and Astronautics

Figure 20: Time history of aircraft state during a 300 *ms*, 50% amplitude aileron right-left doublet.
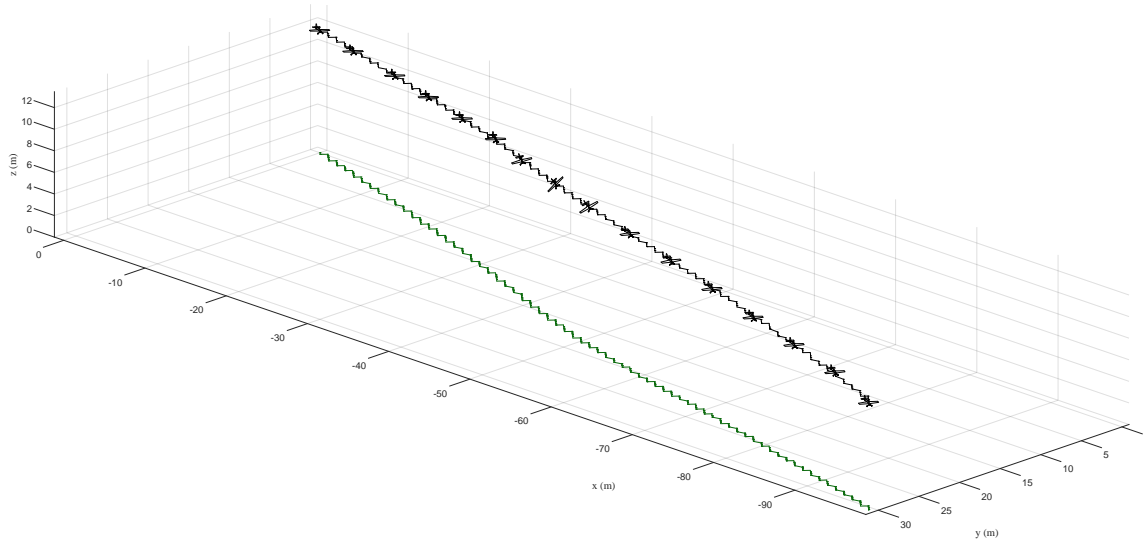
American Institute of Aeronautics and Astronautics

Figure 21: Trajectory of the aircraft during a 300 *ms*, 50% amplitude aileron right-left doublet (the aircraft is drawn once every 0.2 s).

American Institute of Aeronautics and Astronautics

VI.   Summary and Future Work

This paper presented expanded flight and ground testing data sets for the Great Planes Avistar Elite, which are being published on the Unmanned Aerial Vehicle Database. Specifically, ground testing data available includes aircraft 3D scan geometry, moment of inertia measurement, and propeller performance curves. Using this ground testing data, a wealth of digital models were created for the the Great Planes Avistar Elite, including a CAD model in Solidworks, computational aerodynamic models in AVL, XFLR5, and Fluent, a propulsion system power model, and a flight simulation model in X-Plane. Over 50 parameterizable flight testing maneuvers were autonomously performed to characterize aircraft aerodynamics, longitudinal and lateral stability, and control effectiveness; flight test data, state data time histories, and trajectory plots for these maneuvers are available for download.

The Unmanned Aerial Vehicle Database is being expanded to include additional aircraft as they are tested. It is currently planned to test the Great Planes Avistar 30cc, which is an approximately 50% larger version of the Great Planes Avistar Elite presented in this paper, and a 22% scale Cessna 182 Skylane, a geometrically-scaled version of the ubiquitous general aviation aircraft. Additionally, the database will also include geometric and moment of inertia data sets for these aircraft, as well as propulsion system data sets and resulting models. The flight testing of these aircraft is planned to be conducted using the flight testing automation tool, allowing for consistent results.

Acknowledgments

References

[1]Lykins, R. and Keshmiri, S., "Modal Analysis of 1/3-Scale Yak-54 Aircraft Through Simulation and Flight Testing," AIAA Paper 2011-6443, AIAA Atmospheric Flight Mechanics Conference, Portland, Oregon, Aug. 2011.

[2]Johnson, B. and Lind, R., "Characterizing Wing Rock with Variations in Size and Configuration of Vertical Tail," *Journal of Aircraft*, Vol. 47, No. 2, 2010, pp. 567–576.

[3]Perry, J., Mohamed, A., Johnson, B., and Lind, R., "Estimating Angle of Attack and Sideslip Under High Dynamics on Small UAVs," Proceedings of the ION-GNSS Conference, Savannah, Georgia, 2008.

[4]Uhlig, D., Sareen, A., Sukumar, P., Rao, A. H., and Selig, M. S., "Determining Aerodynamic Characteristics of a Micro Air Vehicle Using Motion Tracking," AIAA Paper 2010-8416, AIAA Guidance, Navigation, and Control Conference, Toronto, Ontario, Canada, Aug. 2010.

[5]Dantsker, O. D. and Selig, M. S., "High Angle of Attack Flight of a Subscale Aerobatic Aircraft," AIAA Paper 2015-2568, AIAA Applied Aerodynamics Conference, Dallas, Texas, Jun. 2015.

[6]Mockli, M., *Guidance and Control for Aerobatic Maneuvers of an Unmanned Airplane*, Ph.D. thesis, ETH Zurich, Department of Mechanical and Process Engineering, 2006.

[7]Frank, A., McGrewy, J. S., Valentiz, M., Levinex, D., and How, J. P., "Hover, Transition, and Level Flight Control Design for a Single-Propeller Indoor Airplane," AIAA Paper 2007-6318, AIAA Guidance, Navigation, and Control Conference, Hilton Head, South Carolina, Aug. 2007.

[8]Johnson, E. N., Wu, A. D., Neidhoefer, J. C., Kannan, S. K., and Turbe, M. A., "Test Results of Autonomous Airplane Transitions Between Steady-Level and Hovering Flight," *Journal of Guidance, Control, and Dynamics*, Vol. 31, No. 2, 2008, pp. 358–370.

[9]Johnson, B. and Lind, R., "Trajectory Planning for Sensing Effectiveness with High Angle-of-Attack Flight Capability," AIAA Paper 2012-0276, AIAA Aerospace Sciences Meeting, Nashville, Tennessee, Jan. 2012.

[10]Jordan, T. L. and Bailey, R. M., "NASA Langley's AirSTAR Testbed: A Subscale Flight Test Capability for Flight Dynamics and Control System Experiments," AIAA Paper 2008-6660, AIAA Atmospheric Flight Mechanics Conference, Honolulu, Hawaii, Aug. 2008.

[11]Ragheb, A. M., Dantsker, O. D., and Selig, M. S., "Stall/Spin Flight Testing with a Subscale Aerobatic Aircraft," AIAA Paper 2013-2806, AIAA Applied Aerodynamics Conference, San Diego, California, June 2013.

[12]Bunge, R. A., Savino, F. M., and Kroo, I. M., "Approaches to Automatic Stall/Spin Detection Based on Small-Scale UAV Flight Testing," AIAA Paper 2015-2235, AIAA Atmospheric Flight Mechanics Conference, Dallas, Texas, Jun. 2015.

[13]Ananda, G. K., Vahora, M., Dantsker, O. D., and Selig, M. S., "Design Methodology for a Dynamically-Scaled General Aviation Aircraft," AIAA Paper 2017-4077, AIAA Applied Aerodynamics Conference, Denver, Colorado, June 2017.

[14]Dantsker, O. D., Ananda, G. K., and Selig, M. S., "GA-USTAR Phase 1: Development and Flight Testing of the Baseline Upset and Stall Research Aircraft," AIAA Paper 2017-4078, AIAA Applied Aerodynamics Conference, Denver, Colorado, June 2017.

[15]Risch, T., Cosentino, G., Regan, C., Kisska, M., and Princen, N., "X-48B Flight-Test Progress Overview," AIAA Paper 2009-934, AIAA Aerospace Sciences Meeting, Orlando, FL, Jan. 2009.

[16]Lundstrom, D. and Amadori, K., "Raven: A Subscale Radio Controlled Business Jet Demonstrator," International Congress on the Aeronautical Sciences Systems (ICUAS), Anchorage, Alaska, Sep. 2008.

[17]Regan, C. D. and Taylor, B. R., "mAEWing1: Design, Build, Test - Invited," AIAA Paper 2016-1747, AIAA Atmospheric Flight Mechanics Conference, San Diego, California, Jun. 2016.

[18]Regan, C. D., "mAEWing2: Conceptual Design and System Test," AIAA Paper 2017-1391, AIAA Atmospheric Flight Mechanics Conference, Grapevine, Texas, Jun. 2017.

[19]Leong, H. I., Keshmiri, S., and Jager, R., "Evaluation of a COTS Autopilot and Avionics System for UAVs," AIAA Paper 2009-1963, AIAA Infotech@Aerospace, Seattle, Washington, April. 2009.

[20]Esposito, J. F. and Keshmiri, S., "Rapid Hardware Interfacing and Software Development for Embedded Devices Using Simulink," AIAA Paper 2010-3415, AIAA Infotech@Aerospace, Atlanta, Georgia, June 2010.

[21]Garcia, G. and Keshmiri, S., "Integrated Kalman Filter for a Flight Control System with Redundant Measurements," AIAA Paper 2012-2499, AIAA Infotech@Aerospace, Garden Grove, California, June 2012.

[22].Sobron, A., Lundström, D., Staack, I., and Krus, P., "Design and Testing of a Low-Cost Flight Control and Data Acquisition System for Unstable Subscale Aircraft," International Congress on the Aeronautical Sciences Systems, Daejeon, Korea, Sep. 2016.

[23]Theile, M., Dantsker, O. D., Caccamo, M., and Yu, S., "uavAP: A Modular Autopilot Framework for UAVs," AIAA Paper 2020-3268, AIAA Aviation 2020 Forum, Virtual Event, Jun. 2020.

[24]Sukumar, P. P. and Selig, M. S., "Dynamic Soaring of Sailplanes over Open Fields," *Journal of Aircraft*, Vol. 50, No. 5, Nov.-Dec. 2013, pp. 1420–1430.

[25]Woodbury, T., Dunn, C., and Valasek, J., "Autonomous Soaring Using Reinforcement Learningfor Trajectory Generation," AIAA Paper 2014-0990, AIAA SciTech Forum, National Harbor, Maryland, Jan 2014.

[26]Depenbusch, N. T., Bird, J. J., and Langelaan, J. W., "The AutoSOAR autonomous soaring aircraft, part 1: Autonomy algorithms," *Journal of Field Robotics*, 2016.

[27]Sachs, G. and Gruter, B., "Maximum TravelSpeed Performance of Albatrossesand UAVs Using Dynamic Soaring," AIAA Paper 2019-0568, AIAA SciTech Forum, San Diego, California, Jan 2019.

[28]Bird, J. J. and Langelaan, J. W., "Optimal Speed Scheduling for Hybrid Solar Aircraftwith Arrival Time Condition," AIAA Paper 2019-1421, AIAA SciTech Forum, San Diego, California, Jan 2019.

[29]Keane, A. J., Sóbester, A., and Scanlan, J. P., *Small Unmanned Fixed-Wing Aircraft Design: A Practical Approach*, John Wiley & Sons, United Kingdom, 2017.

[30]Lundstrom, D., *Aircraft Design Automation and Subscale Testing*, Ph.D. thesis, Linkoping University, Department of Management and Engineering, Linkoping, Sweden, 2012.

[31]Dantsker, O. D., *A Cyber-Physical Prototyping and Testing Framework to Enable the Rapid Development of Unmanned Aircraft*, Ph.D. thesis, University of Illinois at Urbana-Champaign, Department of Aerospace Engineering, Urbana, IL, 2021.

[32]Dantsker, O. D., Theile, M., and Caccamo, M., "A Cyber-Physical Prototyping and Testing Framework to Enable the Rapid Development of UAVs," *Aerospace*, Vol. 9, No. 5, 2022.

[33]Hobbico, Inc., "Great Planes Avistar Elite .46 Advanced Trainer RTF," `http://www.greatplanes.com/airplanes/gpma1605.html`, Accessed Oct. 2017.

[34]O. Dantsker and R. Mancuso and M. Vahora and M. Caccamo, "Unmanned Aerial Vehicle Database," `http://uavdb.org/`, Accessed Jan. 2022.

[35]Dantsker, O. D., Yu, S., Vahora, M., and Caccamo, M., "Flight Testing Automation to Parameterize Unmanned Aircraft Dynamics," AIAA Paper 2019-3230, AIAA Aviation and Aeronautics Forum and Exposition, Dallas, Texas, June 2019.

[36]Mancuso, R., Dantsker, O. D., Caccamo, M., and Selig, M. S., "A Low-Power Architecture for High Frequency Sensor Acquisition in Many-DOF UAVs," International Conference on Cyber-Physical Systems, Berlin, Germany, April 2014.

[37]Dantsker, O. D., Mancuso, R., Selig, M. S., and Caccamo, M., "High-Frequency Sensor Data Acquisition System (SDAC) for Flight Control and Aerodynamic Data Collection Research on Small to Mid-Sized UAVs," AIAA Paper 2014-2565, AIAA Applied Aerodynamics Conference, Atlanta, Georgia, June 2014.

[38]Dantsker, O. D., Loius, A. V., Mancuso, R., Caccamo, M., and Selig, M. S., "SDAC-UAS: A Sensor Data Acquisition Unmanned Aerial System for Flight Control and Aerodynamic Data Collection," *AIAA Paper 2015-0987 ,AIAA Infotech@Aerospace Conference, Kissimee, Florida, Jan 2015.*.

[39]Dantsker, O. D., Vahora, M., Imtiaz, S., and Caccamo, M., "High Fidelity Moment of Inertia Testing of Unmanned Aircraft," AIAA Paper 2018-4219, AIAA Applied Aerodynamics Conference, Atlanta, Georgia, Jun. 2018.

[40]Dantsker, O. D., Theile, M., and Caccamo, M., "A High-Fidelity, Low-Order Propulsion Power Model for Fixed-Wing Electric Unmanned Aircraft," AIAA Paper 2018-5009, AIAA/IEEE Electric Aircraft Technologies Symposium, Cincinnati, OH, July 2018.

[41]Dantsker, O. D., Imtiaz, S., and Caccamo, M., "Electric Propulsion System Optimization for a Long-Endurance and Solar-Powered Unmanned Aircraft," AIAA Paper 2019-4486, AIAA/IEEE Electric Aircraft Technologies Symposium, Indianapolis, Indiana, Aug. 2019.

[42]Theile, M., Yu, S., Dantsker, O. D., and Caccamo, M., "Trajectory Estimation for Geo-Fencing Applications on Small-Size Fixed-Wing UAVs," IEEE International Conference on Intelligent Robots and Systems, Macau, China, Nov. 2019.

[43]Al Volo LLC, "Al Volo: Flight Systems," `http://www.alvolo.us`, Accessed Jan. 2022.

[44]Xsens, "MTi-G-710," https://www.xsens.com/mti-g-710, Accessed Dec. 2022.

[45]Dantsker, O. D., "Determining Aerodynamic Characteristics of an Unmanned Aerial Vehicle using a 3D Scanning Technique," AIAA Paper 2015-0026, AIAA Aerospace Sciences Meeting, Kissimmee, Florida, Jan. 2015.

[46]Dantsker, O. D., Caccamo, M., Deters, R. W., and Selig, M. S., "Performance Testing of APC Electric Fixed-Blade UAV Propellers," AIAA Paper 2022-4020, AIAA Aviation Forum, Virtual Event, Jun. 2020.

[47]UIUC Applied Aerodynamics Group, "UIUC Airfoil Coordinates Database," `http://aerospace.illinois.edu/m-selig/ads/coord_database.html`.

[48]Landing Products Inc., "APC Propellers," `https://www.apcprop.com/`, Accessed Jan. 2022.

[49]Bradt, J. B. and Selig, M. S., "Propeller Performance Data at Low Reynolds Numbers," *AIAA Paper 2011-1255 AIAA Aerospace Sciences Meeting, Orlando, Florida, Jan. 2011.*

[50]Brandt, J., Deters, R., Ananda, G., Dantsker, O., and Selig, M., "UIUC Propeller Database," `http://m-selig.ae.illinois.edu/props/propDB.html`, Accessed Jan. 2022.

[51]Dantsker, O. D. and Vahora, M., "Comparison of Aerodynamic Characterization Methods for Design of Unmanned Aerial Vehicles," AIAA Paper 2018-0272, AIAA Aerospace Sciences Meeting, Kissimmee, Florida, Jan 2018.

[52]Andre Deperrois, "XFLR5," `http://www.xflr5.com/`, Accessed Jun. 2017.

[53]Mark Drela, "AVL," `http://web.mit.edu/drela/Public/web/avl/`, Accessed Jan. 2022.

[54]Drela, M., "First-Order DC Electric Motor Model," `http://web.mit.edu/drela/Public/web/qprop/motor1_theory.pdf`.

[55]Green, C. R. and McDonald, R. A., "Modeling and Test of the Efficiency of Electronic Speed Controllers for Brushless DC Motors," AIAA Paper 2015-3191, AIAA Aviation Forum, Dallas, Texas, Jun. 2015.

[56]Gong, A. and Verstraete, D., "Experimental Testing of Electronic Speed Controllers for UAVs," AIAA Paper 2017-4955, AIAA/SAE/ASEE Joint Propulsion Conference, Atlanta, Georgia, July 2017.

[57]Gong, A., MacNeill, R., and Verstraete, D., "Performance Testing and Modeling of a Brushless DC Motor, Electronic Speed Controller and Propeller for a Small UAV," AIAA Paper 2018-4584, AIAA Propulsion and Energy Forum, Cincinnati, Ohio, July 2018.

[58]Laminar Research, "X-Plane 11," `http://www.x-plane.com/`, Accessed Jan. 2022.

[59]Theile, M., Dantsker, O. D., Nai, R., and Caccamo, M., "uavEE: A Modular, Power-Aware Emulation Environment for Rapid Prototyping and Testing of UAVs," IEEE International Conference on Embedded and Real-Time Computing Systems and Applications, Hakodate, Japan, Aug. 2018.